

## Scaling and modelling of turbulence in variable property channel flows

Pecnik, Rene; Patel, Ashish

**DOI**

[10.1017/jfm.2017.348](https://doi.org/10.1017/jfm.2017.348)

**Publication date**

2017

**Document Version**

Accepted author manuscript

**Published in**

Journal of Fluid Mechanics

**Citation (APA)**

Pecnik, R., & Patel, A. (2017). Scaling and modelling of turbulence in variable property channel flows. *Journal of Fluid Mechanics*, 823, Article R1. <https://doi.org/10.1017/jfm.2017.348>

**Important note**

To cite this publication, please use the final published version (if applicable).  
Please check the document version above.

**Copyright**

Other than for strictly personal use, it is not permitted to download, forward or distribute the text or part of it, without the consent of the author(s) and/or copyright holder(s), unless the work is under an open content license such as Creative Commons.

**Takedown policy**

Please contact us and provide details if you believe this document breaches copyrights.  
We will remove access to the work immediately and investigate your claim.

---

# JFM RAPIDS

[journals.cambridge.org/rapids](http://journals.cambridge.org/rapids)

---

## Scaling and modelling of turbulence in variable property channel flows

Rene Pecnik<sup>†</sup>, and Ashish Patel

Process and Energy Department, Delft University of Technology,  
Leegwaterstraat 39, 2628 CB Delft, The Netherlands

(Received xx; revised xx; accepted xx)

---

We derive an alternative formulation of the turbulent kinetic energy equation for flows with strong near-wall density and viscosity gradients. The derivation is based on a scaling transformation of the Navier-Stokes equations using semi-local quantities. A budget analysis of the semi-locally scaled turbulent kinetic energy equation shows that for several variable property low-Mach-number channel flows, the ‘leading-order effect’ of variable density and viscosity on turbulence in wall bounded flows can effectively be characterized by the semi-local Reynolds number. Moreover, if a turbulence model is solved in its semi-locally scaled form, we show that an excellent agreement with direct numerical simulations is obtained for both low- and high-Mach-number flows, where conventional modelling approaches fail.

**Key words:** compressible boundary layers, turbulence modelling, turbulent boundary layers

---

### 1. Introduction

Turbulent flows with variable thermophysical properties are common in nature and engineering applications. For example, the density or viscosity significantly changes in flows of supersonic aircraft, rocket propulsion systems, heat exchangers, chemically reacting flows, or the flow in the Sun’s convection zone. In general, strong thermophysical property variations alter the conventional behaviour of turbulence and cause scaling laws of constant property flows to fail (Bradshaw 1977; Lele 1994; Coleman *et al.* 1995; Duan *et al.* 2010; Lee *et al.* 2013; Modesti & Pirozzoli 2016). From past studies it is known that differences between adiabatic supersonic boundary layers and incompressible isothermal flows can be corrected by simply accounting for mean density variations – an example is the van Driest velocity transformation – as long as the turbulent Mach number remains small,  $M' < 0.3$  (Smits & Dussauge 2006). This is known as Morkovin’s hypothesis (Morkovin 1962). However, for flows with strong wall heat transfer, the van Driest velocity transformation fails to provide a reasonable collapse (Duan *et al.* 2010; Modesti & Pirozzoli 2016). Recently, Trettel & Larsson (2016) and Patel *et al.* (2016) have proposed a transformation that provides a collapse for supersonic channel flows with isothermal

<sup>†</sup> Email address for correspondence: [r.pecnik@tudelft.nl](mailto:r.pecnik@tudelft.nl)

walls, and low-Mach-number volumetrically heated channel flows. Nevertheless, despite the universal scaling law for the mean velocity, it is still not clear how these recent advances can be used to inform models for predicting turbulent statistics. For example, turbulence models still remain incapable to provide reasonable results for wall bounded flows with strong heat transfer (Huang *et al.* 1995; He *et al.* 2008). This has been mostly attributed to effects caused by compressibility, expressed by the dilatational dissipation, pressure work, pressure dilatation and diffusion, etc. Most of these compressible effects, however, remain small in compressible wall bounded flows (Huang *et al.* 1995; Duan *et al.* 2010) and the reason for the failure of turbulence models is yet unknown.

In our recent work (Patel *et al.* 2015), we provided a mathematical basis for the application of semi-local scaling laws as proposed by Huang *et al.* (1995). It was based on rescaling the Navier-Stokes equations using semi-local quantities (e.g., local mean values of density,  $\rho$ , and viscosity,  $\mu$ , etc.), after which an evolution equation for the turbulent velocity fluctuations was derived. In this equation, the viscous terms scale with the semi-local Reynolds number and the production of turbulent fluctuations is governed by the gradient of the density weighted velocity, i.e. the van Driest velocity transformation. The semi-local Reynolds number is defined as

$$Re_\tau^* \equiv \frac{\sqrt{\langle \rho \rangle / \rho_w}}{\langle \mu \rangle / \mu_w} Re_\tau, \quad (1.1)$$

where  $\langle \cdot \rangle$  denotes Reynolds averaging, the subscript  $w$  indicates quantities at the isothermal wall (no averaging at the wall is required) and  $Re_\tau = \rho_w u_{\tau_w} h / \mu_w$  is the friction Reynolds number based on the friction velocity,  $u_{\tau_w}$ , and a characteristic length,  $h$ . The van Driest velocity transformation (in differential form) is given by

$$d\langle u^{vD} \rangle = \sqrt{\langle \rho \rangle / \rho_w} d(\langle u \rangle / u_{\tau_w}). \quad (1.2)$$

Using several direct numerical simulations (DNS) of turbulent channel flows with fluids that have different constitutive relations for density and viscosity, we showed that for cases with similar  $Re_\tau^*$  profiles, similar turbulent statistics are obtained. Moreover, in Patel *et al.* (2016), it was shown that the viscous stress is a universal function in the inner layer, which expressed in semi-local parameters is  $\langle \tau_{(y)} \rangle = 1/Re_\tau^* (d\langle u^{vD} \rangle / dy)$ . Therefore, the van Driest velocity is not an independent quantity and the main parameter that governs turbulence in variable property flows is  $Re_\tau^*$ .

Here, we aim to extend the semi-local scaling framework to derive a semi-locally scaled (SLS) evolution equation for the turbulent kinetic energy (TKE). We will show that also for the SLS TKE equation the viscous terms scale with  $Re_\tau^*$  and the turbulence production is governed by the gradient of the van Driest velocity. We will then use the SLS TKE in conjunction with a turbulence model to simulate several fully developed turbulent flows, ranging from volumetrically heated flows at low Mach (Ma) numbers to a fully compressible Ma=4 case in a channel with isothermal walls provided by Trettel & Larsson (2016).

## 2. The SLS TKE equation

As in Patel *et al.* (2015), we apply a semi-local scaling transformation to the Navier-Stokes equations for density  $\rho$ , dynamic viscosity  $\mu$ , velocity  $u_i$  and pressure  $p$ , defined as

$$\hat{\rho} = \rho / \langle \rho \rangle, \quad \hat{\mu} = \mu / \langle \mu \rangle, \quad \hat{u}_i = u_i / u_\tau^*, \quad \text{and} \quad \hat{p} = p / (\langle \rho \rangle u_\tau^{*2}), \quad (2.1)$$

where  $\langle \rho \rangle$ ,  $\langle \mu \rangle$  and  $u_\tau^*$  are the Reynolds averaged values of local density, local viscosity and semi-local friction velocity  $u_\tau^* = \sqrt{\tau_w / \langle \rho \rangle}$ , with  $\tau_w$  the averaged wall shear stress.

The spatial coordinates are normalized as  $\hat{x} = x/h$ . Applying the scaling transformation to the continuity equation and assuming that the averaged wall shear stress  $\tau_w$  is constant or changes slowly in the streamwise direction, we obtain (cf. Appendix A)

$$t_\tau^* \frac{\partial \hat{\rho}}{\partial t} + \frac{\partial \hat{\rho} \hat{u}_i}{\partial \hat{x}_i} + \hat{\rho} \hat{u}_i \underbrace{\frac{1}{2 \langle \rho \rangle} \frac{\partial \langle \rho \rangle}{\partial \hat{x}_i}}_{d_i} = 0, \quad (2.2)$$

with  $t_\tau^* = h/u_\tau^*$ . The additional term,  $d_i$ , is the result of the semi-local scaling transformation, which contains the gradient of the Reynolds averaged density. Accordingly, the SLS momentum equations in non-conservative form are given as (cf. Appendix B)

$$t_\tau^* \hat{\rho} \frac{\partial \hat{u}_i}{\partial t} + \hat{\rho} \hat{u}_j \frac{\partial \hat{u}_i}{\partial \hat{x}_j} - \hat{\rho} \hat{u}_i \hat{u}_j d_j = - \frac{\partial \hat{p}}{\partial \hat{x}_i} + \frac{\partial \hat{\tau}_{ij}}{\partial \hat{x}_j} - \frac{\partial \hat{D}_{ij}}{\partial \hat{x}_j} + \hat{\rho} \hat{f}_i, \quad (2.3)$$

with the stress tensor  $\hat{\tau}_{ij} = \hat{\mu}/Re_\tau^* [(\partial \hat{u}_i/\partial \hat{x}_j + \partial \hat{u}_j/\partial \hat{x}_i) - 2/3(\partial \hat{u}_k/\partial \hat{x}_k)\delta_{ij}]$ . If compared with the conventional form, two additional terms appear, namely,  $\hat{\rho} \hat{u}_i \hat{u}_j d_j$  and  $\partial_{\hat{x}_j} \hat{D}_{ij}$ , where  $\hat{D}_{ij} = \hat{\mu}/Re_\tau^* [(\hat{u}_i d_j + \hat{u}_j d_i) - 2/3(\hat{u}_k d_k)\delta_{ij}]$ . It should be noted the effective viscosity in  $\hat{\tau}_{ij}$  is proportional to  $1/Re_\tau^*$ .  $\hat{f}_i$  is a normalized arbitrary body force.

Given (2.2) and (2.3), we can now derive the SLS TKE equation using a standard procedure by first multiplying the momentum equation (2.3) with the Favre fluctuating velocity  $\hat{u}_i''$  and then Reynolds averaging the product. To highlight distinct differences in the derivation when using the SLS Navier-Stokes equations, this procedure is outlined for the terms on the left-hand-side of (2.3), while the derivation of the other terms closely follows the standard procedure and is thus not shown. The Favre decomposition is used for the velocity, while the Reynolds decomposition is used for all other quantities, which for an arbitrary quantity  $\phi$  are given as  $\phi = \{\phi\} + \phi''$  and  $\phi = \langle \phi \rangle + \phi'$  respectively. It is important to note that the Favre mean is  $\{\phi\} = \langle \rho \phi \rangle / \langle \rho \rangle$ , which, with the locally scaled density, can also be expressed as  $\{\phi\} = \langle \hat{\rho} \phi \rangle$ ; an identity we will use throughout the derivation of the SLS TKE equation. In addition,  $\langle \hat{\rho} \phi'' \rangle = 0$ .

Multiplying the first term in (2.3) by  $\hat{u}_i''$  and Reynolds averaging the product gives

$$t_\tau^* \left\langle \hat{u}_i'' \hat{\rho} \frac{\partial \hat{u}_i}{\partial t} \right\rangle = t_\tau^* \frac{\partial \langle \frac{1}{2} \hat{\rho} \hat{u}_i'' \hat{u}_i'' \rangle}{\partial t} - \underbrace{\left\langle \hat{k} t_\tau^* \frac{\partial \hat{\rho}}{\partial t} \right\rangle}_{(I)}, \quad (2.4)$$

with the definition of the TKE  $\hat{k} = \hat{u}_i'' \hat{u}_i'' / 2$ . For the convection term, we obtain

$$\left\langle \hat{\rho} \hat{u}_i'' \hat{u}_j \frac{\partial \hat{u}_i}{\partial \hat{x}_j} \right\rangle = \{\hat{u}_i'' \hat{u}_j''\} \frac{\partial \{\hat{u}_i\}}{\partial \hat{x}_j} + \frac{\partial}{\partial \hat{x}_j} \left( \{\hat{u}_j\} \{\hat{k}\} + \{\hat{u}_j'' \hat{k}\} \right) - \underbrace{\left\langle \hat{k} \frac{\partial \hat{\rho}}{\partial \hat{x}_j} \right\rangle}_{(II)}. \quad (2.5)$$

The first term on the right-hand-side of (2.5) represents turbulence production as a function of SLS quantities. As we will see later, it is crucial to express the partial derivative of the SLS mean velocity in terms of the density-weighted partial derivative of velocity using the van Driest transformation given by (1.2). With the additional relation  $\sqrt{\rho_w} u_{\tau_w} = \sqrt{\langle \rho \rangle} u_\tau^*$ , this leads to

$$\frac{\partial \{\hat{u}_i\}}{\partial \hat{x}_j} = \frac{\partial \frac{\{u_i\}}{u_\tau^*}}{\partial \hat{x}_j} = \frac{\partial \sqrt{\frac{\langle \rho \rangle}{\rho_w}} \frac{\{u_i\}}{u_{\tau_w}}}{\partial \hat{x}_j} = \frac{\sqrt{\frac{\langle \rho \rangle}{\rho_w}} \partial \frac{\{u_i\}}{u_{\tau_w}}}{\partial \hat{x}_j} + \frac{\frac{\{u_i\}}{u_{\tau_w}} \partial \sqrt{\frac{\langle \rho \rangle}{\rho_w}}}{\partial \hat{x}_j} = \frac{\partial \{u_i^{vD}\}}{\partial \hat{x}_j} + \{\hat{u}_i\} d_j. \quad (2.6)$$

The turbulence production in (2.5) can then be written as the sum of two terms, namely

$$\{\hat{u}_i''\hat{u}_j''\}\frac{\partial\{\hat{u}_i\}}{\partial\hat{x}_j} = \underbrace{\{\hat{u}_i''\hat{u}_j''\}\frac{\partial\{u_i^{vD}\}}{\partial\hat{x}_j}}_{-\hat{P}_k} + \underbrace{\{\hat{u}_i''\hat{u}_j''\}\{\hat{u}_i\}d_j}_{\text{(III)}}, \quad (2.7)$$

with  $\hat{P}_k$  as the product of Reynolds stress and van Driest velocity gradient, and an additional term (III) that can be large in magnitude, as it is the product of Reynolds stress, Favre averaged velocity and density gradient. However, as we will see later, this term will cancel. The third term in the momentum equation, multiplied by  $\hat{u}_i''$ , gives

$$-\langle\hat{u}_i''\hat{\rho}\hat{u}_i\hat{u}_j\rangle d_j = -\underbrace{\{\hat{u}_i''\hat{u}_j''\}\{\hat{u}_i\}d_j}_{\text{(IV)}} - 2\{\hat{u}_j\}\{\hat{k}\}d_j - 2\{\hat{u}_j''\hat{k}\}d_j. \quad (2.8)$$

We can now proceed and sum the individual terms. For example, the addition of (I) + (II) allows us to substitute the continuity equation (2.2) and we obtain

$$-\left\langle\hat{k}\left(t_\tau^*\frac{\partial\hat{\rho}}{\partial t} + \frac{\partial\hat{\rho}\hat{u}_j}{\partial\hat{x}_j}\right)\right\rangle = \{\hat{u}_j\}\{\hat{k}\}d_j + \{\hat{u}_j''\hat{k}\}d_j. \quad (2.9)$$

As mentioned earlier, term (III) cancels with (IV) since we expressed the velocity gradient in the turbulence production as a function of the van Driest velocity. Summing up all remaining terms, including the conventional decomposition for the pressure and the viscous terms we omitted earlier, results in the SLS TKE equation, given as

$$t_\tau^*\frac{\partial\{\hat{k}\}}{\partial t} + \frac{\partial\{\hat{k}\}\{\hat{u}_j\}}{\partial\hat{x}_j} = \hat{P}_k - \hat{\varepsilon}_k + \hat{T}_k + \hat{C}_k + \hat{D}_k, \quad (2.10)$$

with production  $\hat{P}_k = -\{\hat{u}_i''\hat{u}_j''\}\partial\{u_i^{vD}\}/\partial\hat{x}_j$ , dissipation per unit volume  $\hat{\varepsilon}_k = \langle\hat{\tau}_{ij}'\partial\hat{u}_i'/\partial\hat{x}_j\rangle$ , diffusion (decomposed into viscous diffusion, turbulent transport and pressure diffusion)  $\hat{T}_k = \partial(\langle\hat{u}_i'\hat{\tau}_{ij}'\rangle - \{\hat{u}_j''\hat{k}\} - \langle\hat{p}'\hat{u}_j'\rangle)/\partial\hat{x}_j$ , compressibility  $\hat{C}_k = \langle\hat{p}'\partial\hat{u}_j'/\partial\hat{x}_j\rangle - \langle\hat{u}_j''\rangle\partial\langle\hat{p}\rangle/\partial\hat{x}_j + \langle\hat{u}_i''\rangle\partial\langle\hat{\tau}_{ij}'\rangle/\partial\hat{x}_j$ , and terms related to the mean density gradient  $\hat{D}_k = (\{\hat{u}_j\}\{\hat{k}\} + \{\hat{u}_j''\hat{k}\})d_j - \langle\hat{u}_i''\rangle\partial\hat{D}_{ij}/\partial\hat{x}_j$ . The result is an evolution equation in which the varying density has been absorbed into the van Driest velocity for the production  $\hat{P}_k$ , and the semi-local Reynolds number into the dissipation  $\hat{\varepsilon}_k$  and viscous diffusion. The TKE equation is thus essentially equivalent to its incompressible form, except for the additional terms  $\hat{D}_k$  and  $\hat{C}_k$ , which both can be considered to be small, as we will see later. Since the van Driest velocity is not an independent variable (Patel *et al.* 2016), this derivation suggests that the ‘‘leading order effect’’ on turbulence in variable property flows can be characterized by  $Re_\tau^*$ .

Another intriguing observation is that the TKE equation can be used in its ‘incompressible’ form to model variable property turbulent channel flows. To do so, the velocity in the TKE production term and the viscosity in the viscous terms have to be replaced by the van Driest transformed velocity and the semi-local Reynolds number respectively. Both hypotheses will be tested on flow cases that will be introduced next.

### 3. Turbulent channel flows with variable properties

Table 1 summarises five turbulent channel flows. The first case, CP, corresponds to a reference flow with constant properties at  $Re_\tau = 395$ . The next three cases have been obtained by solving the low-Mach-number approximation of the Navier-Stokes equations, whereby the flows have been volumetrically heated (constant volumetric heat source

Case	$\rho/\rho_w$	$\mu/\mu_w$	$Re_{\tau_w}^*$	$Re_{\tau_c}^*$
CP	1	1	395	395
$CRE_{\tau}^*$	$(T/T_w)^{-1}$	$(T/T_w)^{-0.5}$	395	395
GL (gas-like)	$(T/T_w)^{-1}$	$(T/T_w)^{0.7}$	950	137
LL (liquid-like)	1	$(T/T_w)^{-1}$	150	943
T&L ( $M_b = 4$ )	$\propto p(T/T_w)^{-1}$	$(T/T_w)^{0.75}$	1017	203

TABLE 1. Investigated cases: CP - constant property case with  $Re_{\tau} = 395$ ;  $CRE_{\tau}^*$  - variable property case with constant  $Re_{\tau}^*$  ( $= 395$ ) across the channel; GL - case with gas-like property variations; LL - case with liquid-like property variations; T&L - fully compressible turbulent channel flow with a bulk Mach number of 4 from Trettel & Larsson (2016). The columns report the constitutive relations for density  $\rho$  and viscosity  $\mu$  as a function of temperature  $T$ . The semi-local friction Reynolds numbers at the wall and channel center are given by  $Re_{\tau_w}^*$  and  $Re_{\tau_c}^*$ , respectively.

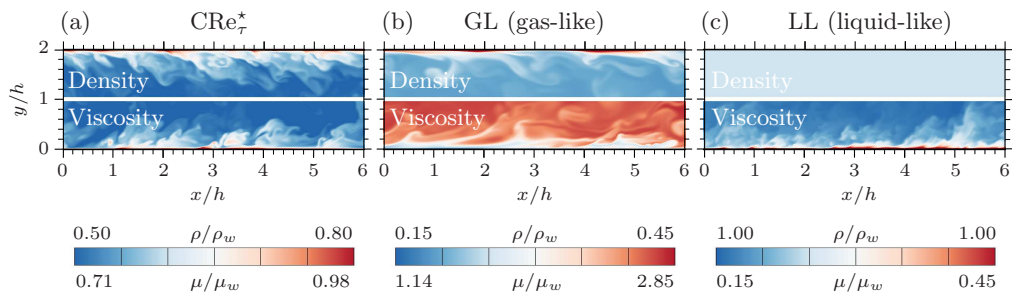


FIGURE 1. Contour plots of instantaneous density  $\rho$  (top half) and dynamic viscosity  $\mu$  (lower half) for cases  $CRE_{\tau}^*$  (a), GL (b), and LL (c).

in the energy equation) and both walls are kept at a constant temperature. Different constitutive relations for density,  $\rho$ , and viscosity,  $\mu$ , as a function of temperature,  $T$ , were used. The case  $CRE_{\tau}^*$  corresponds to a flow for which density and viscosity are decreasing away from the wall (figure 1(a)), such that the semi-local Reynolds number  $Re_{\tau}^*$  is constant across the whole channel height, meaning that  $\sqrt{\langle \rho \rangle} / \rho_w = \langle \mu \rangle / \mu_w$ . Although this case has arbitrary thermophysical properties, it is worthwhile to mention that it bears similarities to supercritical fluids, for which both density and viscosity decrease when heated across the pseudo-critical temperature (Peeters *et al.* 2016; Nemati *et al.* 2016). Cases GL and LL (figure 1(b) and (c)) are flows with gas-like and liquid-like property variations that both have large gradients in  $Re_{\tau}^*$ . More details on the governing equations and the numerical scheme can be found in Patel *et al.* (2015, 2016). The last case in table 1 (case T&L) is a fully compressible turbulent channel flow with isothermal walls, a bulk Mach number of 4 and a wall-based friction Reynolds number of 1017 (Trettel & Larsson 2016).

The largest decrease of density ( $\rho_w / \langle \rho_c \rangle \approx 8.5$ ) is obtained for case  $CRE_{\tau}^*$ , while for cases GL and T&L the density decreases approximately by a factors 5 and 3.6 respectively (figure 2(a)). The profiles for viscosity are shown for the sake of completeness in figure 2(b). However, the most important parameter for the characterization of variable property flows is the semi-local Reynolds number shown in figure 2(c). It can be seen that the cases GL and T&L show similar decreasing  $Re_{\tau}^*$  profiles, while  $Re_{\tau}^*$  for case LL increases. The case  $CRE_{\tau}^*$  has a constant  $Re_{\tau}^*$  profile by construction and collapses with the constant property case CP. The streamwise velocity profiles are shown in figure 2(d-f).

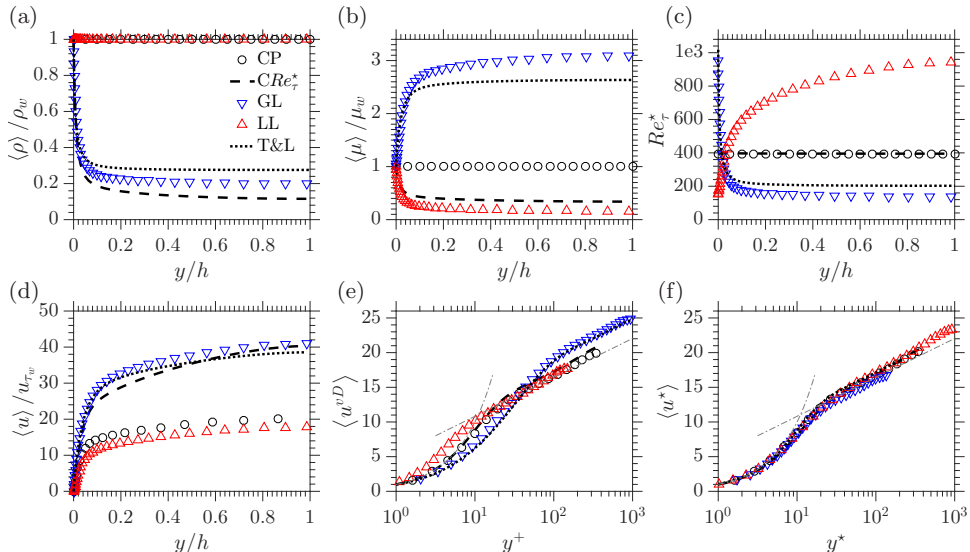


FIGURE 2. Averaged profiles for density (a), viscosity (b), and semi-local Reynolds number (c), velocity (d), van Driest transformed velocity (e), and universal velocity scaling (f) for DNS cases presented in table 1.

It should be noted that, even if the velocity  $\langle u \rangle$  for case  $CRE_\tau^*$  is considerably higher than for case CP, the van Driest velocity transformation is capable of providing a collapse with the constant property universal velocity profile. This is not the case for flows that have gradients in  $Re_\tau^*$  (GL, LL and T&L) since the viscous scales for these cases are changing. On the other hand, the universal velocity scaling proposed by Trettel & Larsson (2016), and later independently derived by Patel *et al.* (2016), provides a good collapse for all cases (figure 2(f)). It should be noted that the normalized wall-normal coordinates are  $y^+ = Re_\tau y/h$ , and  $y^* = Re_\tau^* y/h$ . Since in Patel *et al.* (2016) the universal transformation has been derived by rescaling the Navier–Stokes equations using local mean properties (similarly to the SLS TKE equation), the universal velocity transformation can also be expressed in terms of the van Driest velocity and the semi-local Reynolds number, as  $\langle u^* \rangle = \int_0^{\bar{w}^{vD}} (1 + (y/Re_\tau^*) dRe_\tau^*/dy) d\langle u^{vD} \rangle$ .

#### 4. The SLS TKE budgets

The budget equation for the SLS TKE for fully developed turbulent channel flows can be written as

$$\hat{P}_k - \hat{\varepsilon}_k + \hat{T}_k + \hat{C}_k + \hat{D}_k = 0. \quad (4.1)$$

The budgets for the cases CP,  $CRE_\tau^*$ , GL and LL are shown in figure 3, where they have been scaled by  $Re_\tau^*$ . Despite the large variations in density and viscosity for case  $CRE_\tau^*$ ,  $\hat{P}_k$  and  $\hat{\varepsilon}_k$  are overlapping with case CP (symbols in figure 3a), since for both cases the  $Re_\tau^*$  profiles are constant and equal. This confirms that also turbulence production and dissipation are similar for cases with similar  $Re_\tau^*$  profiles (Patel *et al.* 2015). However, the diffusion is slightly affected by strong property gradients at the location of the production peak at  $y^* \approx 12$ . In general however,  $\hat{C}_k$  and  $\hat{D}_k$  are small for cases  $CRE_\tau^*$  and GL, and for cases CP and LL they are zero, since the density is constant. Based on this observation we can assume that the additional terms,  $\hat{D}_k$  and  $\hat{C}_k$ , have a minor effect on the evolution of the SLS TKE for the cases presented herein. In general, it is accepted that for wall

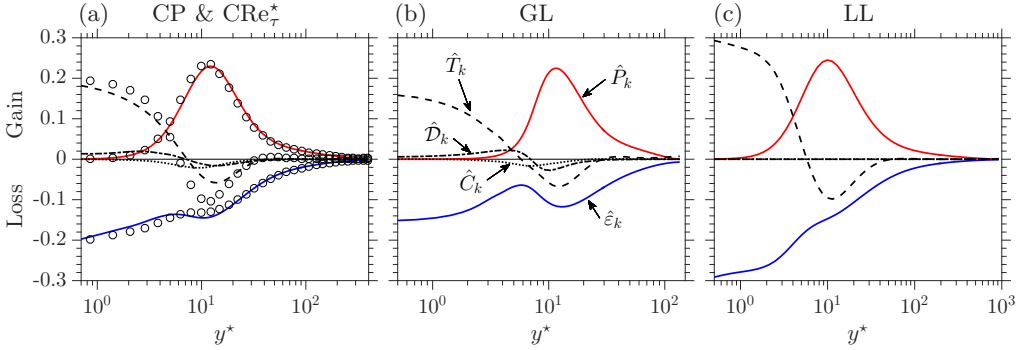


FIGURE 3. Semi-locally scaled turbulent kinetic energy budgets, equation (4.1). (a) case CP (symbols) and  $CRE_\tau^*$  (lines), (b) case GL, and (c) case LL.

bounded flows, the compressibility term  $C_k$  in the traditional budget equation is negligible if compared with the other terms (Morinishi *et al.* 2004; Duan *et al.* 2010).

It should be noted that the key difference, if compared with the conventional semi-local scaling of the budget terms as given in Morinishi *et al.* (2004), Foyssi *et al.* (2004) and Duan *et al.* (2010), is that here we do not scale the individual terms, but we evaluate the budget terms in the TKE equation using SLS variables (e.g.  $\hat{k}$ ,  $\hat{\rho}$ ,  $\hat{\mu}$ , etc.). It is possible to show that for the production, both approaches are equivalent, since  $P_k / (\langle \rho \rangle u_\tau^{*3} / \delta_v^*) = \hat{P}_k / Re_\tau^*$ , with  $\delta_v^* = h / Re_\tau^*$  and  $P_k$  the production term in the traditional TKE equation. However, for the other terms, the conventional semi-local scaling approach and the one presented herein are not equivalent. The SLS TKE equation additionally allows us to clearly distinguish effects related to different distributions of  $Re_\tau^*$  from effects that are reflected in the terms  $\hat{C}_k$  and  $\hat{D}_k$  (in situations where these terms are larger).

## 5. Turbulence modelling

Most turbulence models are based on the  $k - \varepsilon$  model. However, the standard  $k - \varepsilon$  model gives unacceptable results for the turbulent shear stress in the near wall region. Numerous remedies (damping functions, etc.) have been proposed, but these corrections usually negatively affect the accuracy of the modelled TKE. A model that preserves the accuracy of the TKE and also provides accurate results for the turbulent shear stress is the model proposed by Durbin (1995); Lien & Kalitzin (2001). Besides the TKE  $k$  and the dissipation  $\varepsilon$ , this model solves two additional equations, namely a transport equation for the wall normal velocity fluctuation,  $v'^2$ , which is an appropriate velocity scale for turbulent transport towards the wall, and an elliptic relaxation equation that essentially models the pressure strain correlation that appears in the evolution equation of  $v'^2$ . For a fully developed turbulent flow in a channel, the equations for  $k$ ,  $\varepsilon$ ,  $v'^2$  and  $f$  read (the notation of the averaging operators is omitted for brevity)

$$-\partial_y [(\mu + \mu_t / \sigma_k) \partial_y k] = P_k - \rho \varepsilon \quad (5.1)$$

$$-\partial_y [(\mu + \mu_t / \sigma_\varepsilon) \partial_y \varepsilon] = \frac{1}{T} (C_{\varepsilon 1} P_k - C_{\varepsilon 2} \rho \varepsilon) \quad (5.2)$$

$$L^2 \partial_y^2 f - f = \frac{1}{T} [(C_1 - 6) \frac{v'^2}{k} - \frac{2}{3} (C_1 - 1)] - C_2 \frac{P_k}{\rho k} \quad (5.3)$$

$$-\partial_y [(\mu + \mu_t / \sigma_k) \partial_y v'^2] = \rho k f - 6 \rho v'^2 \frac{\varepsilon}{k} \quad (5.4)$$

with  $T = \max(k/\varepsilon, 6\sqrt{\mu/(\rho\varepsilon)})$ ,  $L = 0.23 \max(k^{3/2}/\varepsilon, 70\sqrt{(\mu/\rho)^3/\varepsilon})$  and the eddy viscosity  $\mu_t = C_\mu \rho v'^2 T$ . Using the Boussinesq approximation, the turbulent shear stress is approximated by  $\langle \rho u'' v'' \rangle = -\mu_t \partial_y \langle u \rangle$  and the production can be expressed as



$P_k = \mu_t (\partial_y u)^2$ . The wall boundary condition for the dissipation is  $\varepsilon_w = (\mu_w / \rho_w) \partial_{y^2}^2 k$ , while all other quantities are set to zero. The model coefficients are  $C_\mu = 0.22$ ,  $\sigma_k = 1.0$ ,  $\sigma_\varepsilon = 1.3$ ,  $C_1 = 1.4$ ,  $C_2 = 0.3$ ,  $C_{\varepsilon 1} = 1.4(1 + 0.045\sqrt{k/v'^2})$  and  $C_{\varepsilon 2} = 1.92$ .

The corresponding Reynolds/Favre averaged streamwise momentum equation, using the Boussinesq assumption to approximate the turbulent shear stress, reads

$$\partial_y [(\mu + \mu_t) \partial_y u] = -\rho f_x. \quad (5.5)$$

Since the aim of this study is to investigate the effect of variable properties on turbulent velocity scales, we do not consider the energy equation. Instead we directly prescribe the averaged density and viscosity profiles from DNS. This allows us to study how variable properties affect turbulence, without including compounding errors that originate from modelling the wall-normal turbulent heat flux in the energy equation, commonly approximated by the ratio of the eddy viscosity and the turbulent Prandtl number. It should be noted that if the eddy viscosity is accurately modelled (as we will show below) and the turbulent Prandtl number is constant and known, the energy equation will provide accurate profiles for density and viscosity. Equations (5.1)-(5.5) can be solved to provide approximate solutions of turbulent statistics in variable property channel flows – if the density and viscosity profiles are provided as an input from the DNS.

On the other hand, instead of using the conventional compressible formulation of the turbulence model (5.1)-(5.4), we can solve it in its SLS form. For the channel cases investigated here, we can assume that  $\hat{D}_k$  and  $\hat{C}_k$  can be neglected (see §4). Moreover, following a pragmatic approach, we assume that, analogously to the TKE equation (2.10), the supporting model equations for  $\varepsilon$ ,  $v'^2$  and  $f$  can be expressed in their semi-local formulation as well. We make additionally use of common modelling assumptions, e.g.  $\mu' \ll \langle \mu \rangle$ , and that the molecular and turbulent diffusion can be approximated by the gradient diffusion hypothesis. Then, the only changes that need to be made to solve a turbulence model in its SLS form for fully developed turbulent channel flows are to

- set  $\rho = 1$ ,
- replace  $\mu$  by  $1/Re_\tau^*$  (assuming that  $\mu' \ll \langle \mu \rangle$ , such that  $\hat{\mu} = 1 + \mu' / \langle \mu \rangle \approx 1$ ),
- replace  $\partial u$  in  $P_k$  by  $\partial u^{vD}$
- and, if a model makes use of  $y^+$ , replace it by  $y^*$ .

The corresponding momentum equation can be solved in either its conventional (5.5) or its SLS form, i.e.  $\partial_{\hat{y}} [(1/Re_\tau^* + \hat{\mu}_t) \partial_{\hat{y}} u^{vD}] = -\rho f_x = -1$ . In the latter, it can be seen that, indeed the only parameter that governs the turbulence model and the momentum equation is  $Re_\tau^*$ . If the momentum equation is solved in its conventional form, the SLS eddy viscosity  $\hat{\mu}_t$ , which is provided by the turbulence model, has to be transformed to the conventionally scaled form by  $\mu_t = \langle \rho \rangle h u_\tau^* \hat{\mu}_t$ . This relation can be obtained using the same normalization as introduced in (2.1). Nevertheless, it can be shown that both formulations of the momentum equation lead to equivalent results.

The results of the conventional compressible form and the SLS form are presented in figure 4 and compared with results from the DNS. Evidently, in contrast to the conventional formulation of the turbulence model, the SLS formulation significantly improves the results. For example, the conventional model fails to provide reasonable results, even for a case with constant  $Re_\tau^*$  (case CRe $_\tau^*$ ), which, compared with case CP, has quasi-similar profiles of the viscous scales (see Patel *et al.* (2016)) and the SLS budgets (figure 3). Moreover, for case GL and the supersonic turbulent channel flow case T&L the results with the SLS formulation improve considerably. In particular, the velocity  $\langle u^* \rangle$  and  $\{\hat{k}\}$  close to the wall (row 1 and 3) show a very good agreement with DNS. Since

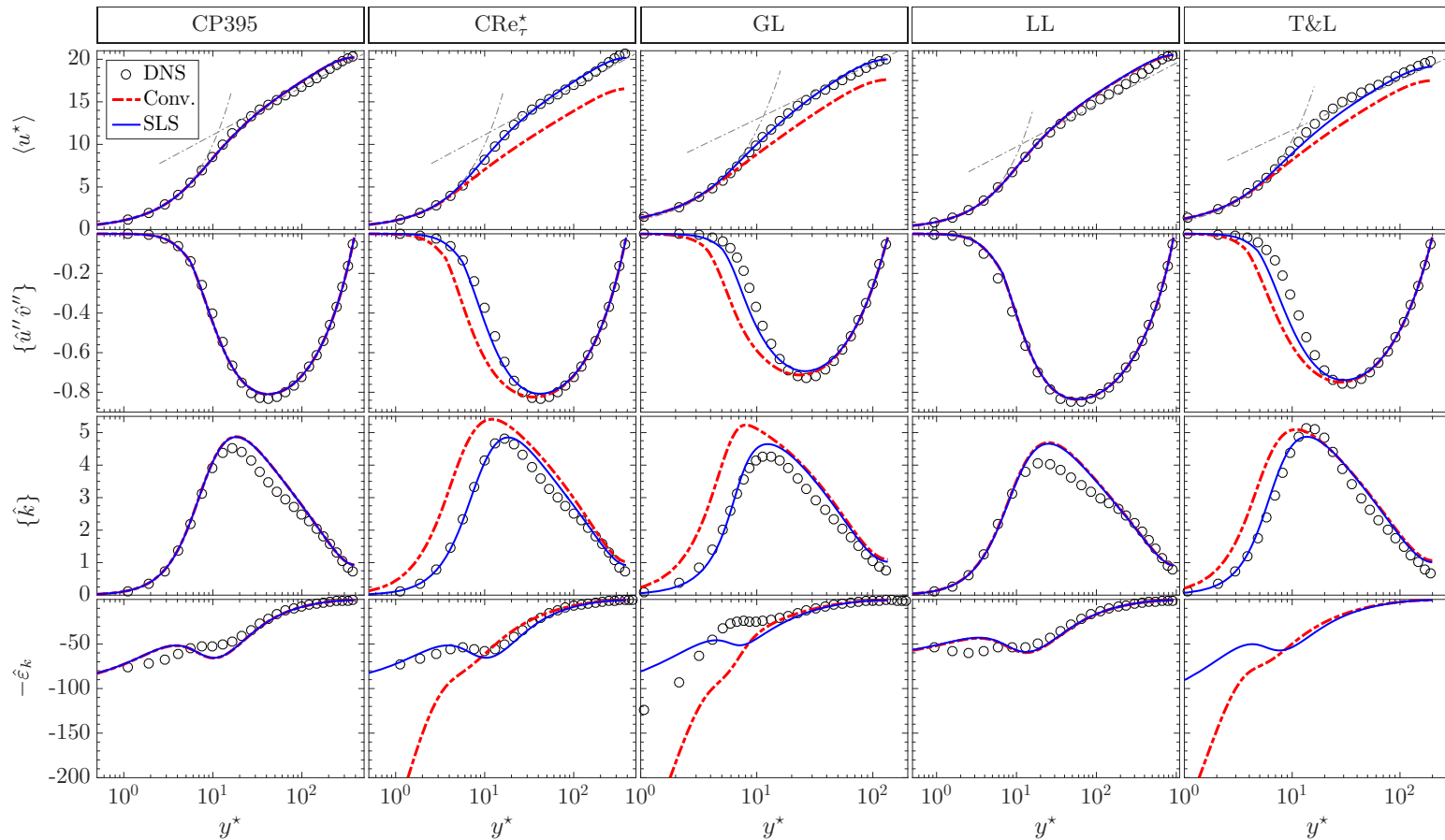


FIGURE 4. DNS results (symbols) compared to conventional (red dash-dotted line) and semi-locally scaled turbulence model (blue solid line) for the cases (columns) introduced in table 1. The rows correspond to the universal velocity transformation  $\langle u^* \rangle$ , semi-locally scaled profiles for turbulent shear stress  $\{\hat{u}'' \hat{v}''\}$ , turbulent kinetic energy  $\{k\}$  and dissipation  $\hat{\epsilon}$ .  $\hat{\epsilon}$  (semi-locally scaled) from DNS for case T&L was not available to the authors.

the density is constant for case LL, both approaches give equivalent result and agree well with DNS.

## 6. Conclusion

In summary, we have derived an alternative form of the TKE equation for wall bounded flows with strong near-wall density and viscosity variations, which is based on a simple scaling transformation of the Navier-Stokes equations using semi-local quantities. The resulting SLS evolution equation clearly indicates that the ‘leading-order effect’ of variable properties on turbulence can distinctively be characterized by the semi-local Reynolds number, and that higher-order effects, such as solenoidal dissipation, pressure-work, -diffusion and -dilatation, are indeed small and that they play a minor role in modulating turbulence for the cases investigated herein. Moreover, if a turbulence model is solved in its SLS form, instead of its conventional compressible form, we showed that an excellent agreement with DNS can be obtained. We anticipate that the formulation of the SLS turbulent kinetic energy, also has the potential to allow for better characterizations and improved turbulence modelling of more complex flow configurations, such as developing supersonic boundary layers, or strongly heated or cooled flows with fluids close to their vapour-liquid critical point. Yet, this will have to be explored in future studies, especially for general geometries.

We thank Andrew Trettel and Johan Larsson for kindly providing data for the supersonic turbulent channel flow. We also acknowledge the access to large scale computing facilities from the Netherlands Organisation for Scientific Research (NWO) through the grant with the dossier number SSH-223-13.

## Appendix A. Derivation of the SLS continuity equation

By applying the scaling transformation to the continuity equation, we may write

$$\frac{\partial \langle \rho \rangle \hat{\rho}}{\partial t} + \frac{\partial (\langle \rho \rangle \hat{\rho} u_\tau^* \hat{u}_i)}{h \partial \hat{x}_i} = \langle \rho \rangle \frac{\partial \hat{\rho}}{\partial t} + \frac{\langle \rho \rangle u_\tau^*}{h} \frac{\partial \hat{\rho} \hat{u}_i}{\partial \hat{x}_i} + \frac{\hat{\rho} \hat{u}_i}{h} \frac{\partial \langle \rho \rangle u_\tau^*}{\partial \hat{x}_i} = 0. \quad (\text{A } 1)$$

With the definition of the semi-local friction velocity  $u_\tau^* = \sqrt{\tau_w / \langle \rho \rangle}$  and with the assumption that the averaged wall shear stress  $\tau_w$  is constant (valid for fully developed channel flows), or that  $\tau_w$  changes slowly in streamwise direction, the spatial derivative in the last term of (A 1) can be written as

$$\frac{\partial \langle \rho \rangle u_\tau^*}{\partial \hat{x}_i} = \sqrt{\tau_w} \frac{\partial \sqrt{\langle \rho \rangle}}{\partial \hat{x}_i} = \sqrt{\tau_w} \frac{\partial \sqrt{\langle \rho \rangle}}{\partial \langle \rho \rangle} \frac{\partial \langle \rho \rangle}{\partial \hat{x}_i} = \frac{1}{2} \frac{\sqrt{\tau_w}}{\sqrt{\langle \rho \rangle}} \frac{\partial \langle \rho \rangle}{\partial \hat{x}_i} = \frac{1}{2} u_\tau^* \frac{\partial \langle \rho \rangle}{\partial \hat{x}_i}. \quad (\text{A } 2)$$

Substituting the final expression of (A 2) into (A 1), and multiplying the result by  $h / (\langle \rho \rangle u_\tau^*)$ , gives the semi-locally scaled continuity equation (2.2).

## Appendix B. Derivation of the SLS momentum equation

By applying the scaling transformation to the non-conservative form of the momentum equation, we may write

$$\langle \rho \rangle u_\tau^* \hat{\rho} \frac{\partial \hat{u}_i}{\partial t} + \langle \rho \rangle u_\tau^* \hat{\rho} \hat{u}_j \frac{\partial u_\tau^* \hat{u}_i}{h \partial \hat{x}_j} = - \frac{\partial \langle \rho \rangle u_\tau^{*2} \hat{p}}{h \partial \hat{x}_i} + \frac{\partial \sigma_{ij}}{h \partial \hat{x}_j} + \langle \rho \rangle \hat{\rho} f_i, \quad (\text{B } 1)$$

with  $\sigma_{ij} = \langle \mu \rangle \hat{\mu} / h [(\partial(u_\tau^* \hat{u}_i) / \partial \hat{x}_j + \partial(u_\tau^* \hat{u}_j) / \partial \hat{x}_i) - 2/3 (\partial(u_\tau^* \hat{u}_k) / \partial \hat{x}_k) \delta_{ij}]$  and  $f_i$  an arbitrary body force. Again making use of the assumption that  $\tau_w$  is constant, it is

first convenient to express the spatial gradient of  $u_\tau^*$  as

$$\frac{\partial u_\tau^*}{\partial \hat{x}_i} = \sqrt{\tau_w} \frac{\partial \sqrt{1/\langle \rho \rangle}}{\partial \hat{x}_i} = \sqrt{\tau_w} \frac{\partial \sqrt{1/\langle \rho \rangle}}{\partial \langle \rho \rangle} \frac{\partial \langle \rho \rangle}{\partial \hat{x}_i} = -\frac{1}{2} \frac{u_\tau^*}{\langle \rho \rangle} \frac{\partial \langle \rho \rangle}{\partial \hat{x}_i} = -u_\tau^* d_i, \quad (\text{B } 2)$$

with  $d_i = \partial_{\hat{x}_i} \langle \rho \rangle / (2 \langle \rho \rangle)$ . Now, applying the product rule for the spatial derivative in the advection term (second term in (B 1)) and using the result of (B 2), we can write

$$\langle \rho \rangle u_\tau^* \hat{\rho} \hat{u}_j \frac{\partial u_\tau^* \hat{u}_i}{h \partial \hat{x}_j} = \frac{\langle \rho \rangle u_\tau^{*2}}{h} \left( \hat{\rho} \hat{u}_j \frac{\partial \hat{u}_i}{\partial \hat{x}_j} - \hat{\rho} \hat{u}_i \hat{u}_j d_j \right). \quad (\text{B } 3)$$

In a similar fashion, we may also use the product rule for the derivatives in  $\hat{\sigma}_{ij}$  and use (B 2) to obtain

$$\sigma_{ij} = \frac{\langle \mu \rangle \hat{\mu} u_\tau^*}{h} \left[ \frac{\partial \hat{u}_i}{\partial \hat{x}_j} + \frac{\partial \hat{u}_j}{\partial \hat{x}_i} - \frac{2}{3} \frac{\partial \hat{u}_k}{\partial \hat{x}_k} \delta_{ij} - \left( \hat{u}_i d_j + \hat{u}_j d_i - \frac{2}{3} \hat{u}_k d_k \delta_{ij} \right) \right]. \quad (\text{B } 4)$$

Making use of (B 3) and (B 4), multiplying (B 1) by  $h/(\langle \rho \rangle u_\tau^{*2})$ , and considering that  $\langle \rho \rangle u_\tau^{*2} = \tau_w$  (such that it can be moved across derivatives), one obtains the SLS momentum equation (2.3), where the viscous stresses (B 4) are scaled by  $1/Re_\tau^*$ , with  $Re_\tau^* = \langle \rho \rangle u_\tau^* h / \langle \mu \rangle$ . Note, the arbitrary forcing is normalized as  $\hat{f}_i = f_i (h/u_\tau^{*2})$ .

## References

- BRADSHAW, P. 1977 Compressible turbulent shear layers. *Annual Review of Fluid Mechanics* **9** (1), 33–52.
- COLEMAN, G. N., KIM, J. & MOSER, R. D. 1995 A numerical study of turbulent supersonic isothermal-wall channel flow. *J. Fluid Mech.* **305**, 159–183.
- DUAN, L., BEEKMAN, I. & MARTIN, M. P. 2010 Direct numerical simulation of hypersonic turbulent boundary layers. Part 2. Effect of wall temperature. *J. Fluid Mech.* **655**, 419–445.
- DURBIN, P. A. 1995 Separated flow computations with the k-epsilon-v-squared model. *AIAA journal* **33** (4), 659–664.
- FOYSI, H., SARKAR, S. & FRIEDRICH, R. 2004 Compressibility effects and turbulence scalings in supersonic channel flow. *J. Fluid Mech.* **509**, 207–216.
- HE, S., KIM, W. & BAE, J. 2008 Assessment of performance of turbulence models in predicting supercritical pressure heat transfer in a vertical tube. *International Journal of Heat and Mass Transfer* **51** (19), 4659–4675.
- HUANG, P. G., COLEMAN, G. N. & BRADSHAW, P. 1995 Compressible turbulent channel flows: DNS results and modelling. *J. Fluid Mech.* **305**, 185–218.
- LEE, J., YOON JUNG, S., JIN SUNG, H. & ZAKI, T. A. 2013 Effect of wall heating on turbulent boundary layers with temperature-dependent viscosity. *J. Fluid Mech.* **726**, 196–225.
- LELE, S. K. 1994 Compressibility effects on turbulence. *Annual review of fluid mechanics* **26** (1), 211–254.
- LIEN, F.-S. & KALITZIN, G. 2001 Computations of transonic flow with the v2-f turbulence model. *International Journal of Heat and Fluid Flow* **22** (1), 53 – 61.
- MODESTI, D. & PIROZZOLI, S. 2016 Reynolds and Mach number effects in compressible turbulent channel flow. *Intl J. Heat Fluid Flow* **59**, 33–49.
- MORINISHI, Y., TAMANO, S. & NAKABAYASHI, K. 2004 Direct numerical simulation of compressible turbulent channel flow between adiabatic and isothermal walls. *J. Fluid Mech.* **502**, 273–308.
- MORKOVIN, M. V. 1962 Effects of compressibility on turbulent flows. *Mecanique de la Turbulence* pp. 367–380.
- NEMATI, H., PATEL, A., BOERSMA, B. J. & PECNIK, R. 2016 The effect of thermal boundary conditions on forced convection heat transfer to fluids at supercritical pressure. *Journal of Fluid Mechanics* **800**, 531–556.

- PATEL, A., BOERSMA, B. J. & PECNIK, R. 2016 The influence of near-wall density and viscosity gradients on turbulence in channel flows. *J. Fluid Mech.* **809**, 793–820.
- PATEL, A., PEETERS, J. W. R., BOERSMA, B. J. & PECNIK, R. 2015 Semi-local scaling and turbulence modulation in variable property turbulent channel flows. *Phys. Fluids* **27** (9), 095101.
- PEETERS, J. W., PECNIK, R., ROHDE, M., VAN DER HAGEN, T. & BOERSMA, B. 2016 Turbulence attenuation in simultaneously heated and cooled annular flows at supercritical pressure. *Journal of Fluid Mechanics* **799**, 505–540.
- SMITS, A. J. & DUSSAUGE, J.-P. 2006 *Turbulent shear layers in supersonic flow*. Springer Science & Business Media.
- TRETTEL, A. & LARSSON, J. 2016 Mean velocity scaling for compressible wall turbulence with heat transfer. *Physics of Fluids (1994-present)* **28** (2), 026102.